Towards predictive understanding of regional climate change

Shang-Ping Xie[1]*, Clara Deser[2], Gabriel A. Vecchi[3], Matthew Collins[4], Thomas L. Delworth[3], Alex Hall[5], Ed Hawkins[6], Nathaniel C. Johnson[7,1,8], Christophe Cassou[9], Alessandra Giannini[10] & Masahiro Watanabe[11]

Regional information on climate change is urgently needed but often deemed unreliable. To achieve credible regional climate projections, it is essential to understand underlying physical processes, reduce model biases and evaluate their impact on projections, and adequately account for internal variability. In the tropics, where atmospheric internal variability is small compared to the forced change, advancing our understanding of the long-term coupling between changes in upper ocean temperature and the atmospheric circulation will help most to narrow uncertainty. In the extratropics, relatively large internal variability introduces substantial uncertainty, while exacerbating risks associated with extreme events. Large ensemble simulations are essential to estimate the probabilistic distribution of climate change on regional scales. We conclude that the current priority is to understand and reduce uncertainties on scales > 100 km to facilitate assessments at finer scales.

(5557 words in text, 134 words for preface)

[1]Scripps Institution of Oceanography, University of California San Diego, 9500 Gilman Drive, La Jolla, CA 92093-0206, USA. [2]National Center for Atmospheric Research, Boulder, CO 80307-3000, USA. [3]Geophysical Fluid Dynamics Laboratory, 201 Forrestal Road, Princeton, NJ 08540-6649, USA. [4]College of Engineering, Mathematics and Physical Sciences, University of Exeter, Exeter, EX4 4QF, UK. [5]Department of Atmospheric and Oceanic Sciences, UCLA, 405 Hilgard Ave., Los Angeles, CA 90095, USA. [6]National Centre for Atmospheric Science**,** Department of Meteorology, University of Reading, Reading, RG6 6BB, UK. [7]International Pacific Research Center, University of Hawaii at Manoa, Honolulu, HI 96822, USA. [8]Cooperative Institute for Climate Science, Princeton University, Princeton, NJ 08540, USA. [9]CNRS/CERFACS, 42 avenue Gaspard Coriolis, Toulouse F-31057 Cedex, France. [10]International Research Institute for Climate and Society, Columbia University, 61 Route 9W, Palisades, NY 10964-8000, USA. [11]Atmosphere and Ocean Research Institute, University of Tokyo, 5-1-5 Kashiwanoha, Kashiwa, Chiba 277-8568, Japan. *e-mail: sxie@ucsd.edu

1. Introduction

Climate change is one of the most serious challenges facing humanity, and extends far beyond the rise in global mean temperatures. Regional manifestations of climate change, including changes in droughts, floods, storminess, wildfires and heat waves, will affect societies and ecosystems. Information about regional impacts is crucial to support planning in many economic sectors, including agriculture, energy, and water resources. Despite their importance, reliable projections of regional climate change face ongoing challenges[1].

Here we review recent advances in understanding regional climate change, offer a critical discussion of outstanding issues, and make recommendations for future progress. We start by highlighting robust regional climate change patterns and their physical underpinnings, with a focus on temperature, precipitation and atmospheric circulation (Section 2). Next we discuss outstanding challenges, including those related to physical understanding, model biases, and internal variability effects, all of which contribute to uncertainty in projected changes of regional climate and extreme events (Section 3). We conclude with a perspective on emerging opportunities in regional climate change research, including efforts to better understand and quantify projections of extreme events enabled by increasing model resolution and ensemble size.

2. Mechanisms for regional climate change

Regional climate projections are often perceived as synonymous with downscaling, but a better understanding of the physical origins of regional changes is essential to achieve more reliable projections. Regional models and global climate models (GCMs) alike can facilitate this understanding. Here we use the term "regional" in a broad sense, considering scales as large as whole continents and ocean basins (1000s of km) or as small as a few hundred km, limited by the resolution of GCMs and long historical observations. Regional models can achieve finer resolution.

Climate anomalies are made up of a response to radiative changes and variability generated internally within the ocean-atmosphere-land-cryosphere system. Projections rely on assumptions about future changes in greenhouse gases (GHGs), aerosols and land-use. Radiative forcing will probably continue increasing for the rest of the century, though the rate of increase is uncertain. Over time, the forced response will strengthen, diminishing internal

variability's relative contribution. Unless aggressive mitigation policies curb GHG emissions, the forced response is expected to dominate regional temperature change by century's end[2].

Uncertainty in regional climate projections arises from internal variability and differences in model structure and forcing scenario, with the relative importance of these factors varying with time horizon[3]. This section highlights robust patterns of regional climate change while Section 3 discusses uncertainties due to model biases and internal variability. GHG forcing uncertainty will not be treated in detail since at the regional scale it can be nearly eliminated simply by scaling with global mean temperature change. However, aerosols are an important regional-scale forcing, and their imprint on regional climate change patterns will be discussed.

2.1 Temperature

For timescales of a century and longer, the magnitude of global mean temperature change under any emissions scenario is related to the Equilibrium Climate Sensitivity (ECS)[4] and the rate of deep oceanic heat uptake, which determines how quickly ECS is approached. Different models produce different values of these key metrics. A GCM's ECS can be approximated as the sum of albedo, water vapour, lapse rate and cloud feedbacks. Cloud feedback is the dominant source of model spread[5]. Such feedbacks are strongly related to regional phenomena, so that the global mean is determined by integrated regional-scale effects (e.g., ice albedo feedback).

At continental scales, robust features of surface air temperature change have been found in observations and model projections (Fig. 1a). Polar amplification is a hallmark of surface temperature change in the Northern Hemisphere. It is largely a consequence of sea ice and snow albedo feedbacks, though poleward energy transport and feedbacks from clouds and water vapour may also be important[6,7]. The ratio of land warming to ocean warming is found to be greater than unity across all scenarios and models for both transient and equilibrium warming, due to differences in surface sensible and latent heat fluxes, boundary layer lapse rate and relative humidity, and cloud cover[8]. Muted warming is found in the Southern Ocean where excess surface heat is mixed into the ocean interior more effectively[9,10]. A similar feature is found in the North Atlantic subpolar gyre. These large-scale features are amenable to 'pattern scaling', where fixed surface temperature change patterns are scaled by the global mean temperature response across scenarios and through time[11].

2.2 Precipitation

While surface temperatures rise everywhere in future projections, precipitation change is highly variable spatially in sign and amplitude, with a relatively small global mean change (Fig. 1). The fundamentally regional character of forced precipitation change highlights the challenge for predicting precipitation.

In the absence of major circulation changes, atmospheric moisture increases with warming, strengthening the climatological distribution of precipitation minus evaporation (P-E) [12,13]. This explains the general rainfall increase in summer monsoon regions[14], for example. At high latitudes, precipitation increases as storms transport more moisture poleward[15]. Over tropical oceans, the wet-gets-wetter pattern is realized in atmospheric models in the idealized case where sea surface warming is spatially uniform (Fig. 2a).

Spatial patterns of sea surface temperature (SST) changes affect tropical convection. Fast equatorial waves flatten horizontal temperature gradients in the tropical free troposphere, so that convective instability, measured by the moist static energy difference between the surface and upper troposphere, largely follows the SST pattern. As a result, tropical rainfall change follows a warmer-gets-wetter pattern (i.e., positive where the local warming exceeds the tropical average)[16]. Enhanced warming over the equatorial Pacific and Atlantic anchors a band of rainfall increase where rainfall is currently low (Figs. 1b, 2b). Ocean-atmosphere feedback is important in coupled SST-rainfall pattern formation. For example, muted surface warming in the tropical Southeast Pacific is associated with acceleration of the southeast trade winds, which suppresses the rainfall increase along the southeastward slanted rain band called the South Pacific Convergence Zone (Fig. 2)[17]. The equatorial peak in SST warming is a robust feature across models due to reduced evaporative damping[18]. The ongoing decadal cooling of the equatorial Pacific[19] is, however, a sober reminder of the difficulty in detecting anthropogenically forced ocean warming patterns amidst internal variability.

Competing effects of moisture and circulation change on P-E can be understood by decomposing the P-E response into a thermodynamic component due to moisture increase with no circulation change, and a dynamic component due to circulation change with no moisture change. The thermodynamic component gives rise to the wet-gets-wetter effect, but overestimates it because of partial compensation by the tropical circulation slowdown[15,20]. Sea

surface warming patterns induce atmospheric circulation change, so that the warmer-gets-wetter effect is part of the dynamic component. While SST patterns do not change much through the year, the thermodynamic component strengthens in the rainy season, and wet regions in the rainy season tend to get wetter[21].

In monsoon regions, precipitation is concentrated in the summer season. Summertime monsoon rains are projected to intensify due to moisture increase, a change especially pronounced for the Asian-Australian monsoons[14]. A robust shift in the seasonal cycle is apparent in GCMs, characterized by a delay in monsoon onset and an increase in precipitation later in the season[22]. The delay in onset is consistent with a vertical stability increase, similar to a developing El Niño event[23]. This effect is compensated by a later increase in moisture convergence[24]. Over tropical continents, remote oceanic influence on rainfall changes is also important[25]. Over the African Sahel, for example, precipitation change follows the SST difference between the neighboring subtropical North Atlantic and global tropics[26].

Relatively high consistency in rainfall change emerges over tropical oceans from model projections (Fig. 1b), but large inter-model variability remains (Fig. 3a). Decomposition of inter-model variability shows that the dynamic component (due to uncertainties in atmospheric circulation change) dominates the uncertainty (Fig. 3b). The inter-model variability in tropical circulation can be traced further to differences in sea surface warming patterns. For example, an anomalous inter-hemispheric Hadley cell tied to a cross-equatorial SST gradient dominates the inter-model variability in the zonal mean. This displaces the band of increased rainfall into the anomalously warm hemisphere[27]. The SST pattern effect has also been identified in inter-model variability of rainfall change in the Sahel[26] and Amazon[28,29] though land surface feedback is also important in these cases. In the tropics, the tight relationship between circulation uncertainties and SST patterns points to the importance of ocean-atmosphere interaction. Ultimately, the coupled SST-circulation uncertainty originates from parameterized physics such as convection, land surface processes and aerosol effects.

2.3 Circulation

As climate warms, atmospheric moisture content increases at a rate of 6-7% per degree warming, set by the Clausius-Clapeyron equation. The global mean precipitation increase is much less (2-3% K^{-1}) because it is constrained by tropospheric radiative cooling[13]. The

difference between these rates of increase is consistent with a general decrease in the tropical overturning circulation[13]. In climate model projections, the east-west Walker circulation shows such a robust slowdown[30], but changes in the north-south Hadley circulation strength are more varied and depend on the cross-equatorial ocean warming gradient[27]. In addition, the Hadley circulation expands poleward[31]. What determines its poleward expansion has not been fully explained, but relates to the latitude at which the associated westerly flow becomes baroclinically unstable[31]. The expansion coincides with poleward shifts in arid zones, with important implications in sensitive regions (e.g., the Mediterranean climate zones)[32,33]. It is also consistent with an intensification of summertime subtropical anticyclones[34].

Aerosol forcing is an important driver of atmospheric circulation change. Unlike GHGs, anthropogenic aerosols are geographically distributed because of their short atmospheric residence time (~a week), with high concentrations in the source regions of southeastern Asia, Europe and the Americas. Because of their strong spatial gradients, anthropogenic aerosols induce atmospheric circulation change more effectively than GHGs per unit radiative forcing[35]. Larger in the Northern Hemisphere, aerosol forcing generates an anomalous Hadley circulation that displaces tropical rainfall into the relatively warm Southern Hemisphere[36]. A striking regional manifestation of this aerosol effect is the precipitation decline in the African Sahel from the 1950s to the 1980s[37,38]. Over the Asian monsoon region, model results show that aerosol-induced cooling drives a divergent circulation in the lower troposphere. This dominates over the thermodynamic effect of GHG-induced temperature increase, causing monsoon rainfall to decrease over the 20th century[39].

Despite their distinct geographical distributions, aerosols and GHGs induce surprisingly similar patterns of SST and oceanic precipitation change[40]. Such robust macro-structures emerge despite large uncertainties in representing micro-physical aerosol effects[41]. This is because the climate system adjusts to radiative forcing through common ocean-atmospheric feedbacks that imprint characteristic patterns on the response. Because GHG and aerosol forcings oppose one another, and because aerosols are more effective per unit forcing in inducing atmospheric circulation and precipitation response, 20th century tropical rainfall change is relatively small and hard to detect. However, future changes may differ as anthropogenic aerosol loading is projected to decline, while the GHG signal is projected to continue growing.

In the Southern Hemisphere, GHG forcing causes the westerly wind jets and stormtracks to shift poleward in association with the increased equator-to-pole temperature gradient in the upper troposphere[42,43]. Ozone depletion in the southern polar stratosphere also contributes to poleward movement of the westerly jets and changes in subtropical precipitation patterns[44]. Forced changes in the Northern Hemisphere westerly jets are less pronounced. Compared to the tropics, coupling between large-scale atmospheric circulation and the SST pattern is weak in the extratropics. Atmospheric internal variability is also large, making it difficult to isolate the forced response. Finally, non-linear interactions between the mean flow and weather systems create blocking events, which are poorly understood and may be inadequately represented by models. Shepherd[45] reviews mid-latitude atmospheric dynamics related to climate change.

2.4 El Niño

The above discussion relates to changes in mean climate, but large-scale modes of internal variability greatly affect regional weather and climate over a broad temporal spectrum, from daily extremes to decadal changes. Their possible alteration in both frequency and amplitude under climate change is a key source of uncertainty at the regional scale.

In the tropics, El Niño-Southern Oscillation (ENSO) is the dominant source of fluctuations in present climate and is expected to remain so[14]. Despite common future changes in mean states potentially affecting ENSO growth, e.g., equatorial trade wind weakening and shoaling of the thermocline[30], climate models do not show any systematic change in the typical amplitude of east Pacific SST variations[46,47]. The spread among model responses is likely due to systematic errors in simulating present-day ENSO[48]. In addition, there is a delicate balance between amplifying and decaying feedbacks in the ENSO cycle, and their relative modifications by climate change differ among models[49,50]. Low-frequency ENSO modulation, independent of radiative forcing changes, also makes detection of the anthropogenic response a challenge[51]. Nevertheless, there is increasing evidence that ENSO properties besides SST amplitude will change robustly due to the patterned background SST increase. For instance, positive rainfall anomalies during ENSO warm phases over the central equatorial Pacific will intensify[52,53] because locally enhanced surface warming reduces the barrier to atmospheric convection. In turn, more frequent extreme tropical rainfall events during El Niño may affect weather patterns worldwide via atmospheric teleconnections. Associated with the enhanced

convective response over the eastern equatorial Pacific, the ENSO-forced Pacific North American pattern tends to intensify and shift eastward in a warmer climate[14].

2.5 Extremes

Changes in temperature extremes often scale with changes in the mean[54,55], indicating local temperature variance has changed little throughout the globe[56]. However, variance in individual climate realizations may change under continued global warming, altering tails of probability distributions and frequencies of extreme events. Such projected changes include reduced wintertime mid- and high-latitude temperature variability owing to Arctic amplification[57] and increased summertime temperature variability in some midlatitude regions owing to soil moisture feedback[58].

Precipitation intensity is projected to increase globally. Water vapor increases contribute most strongly to these changes in the tropics, but atmospheric circulation changes also play a role in midlatitudes[59]. For example, the projected poleward shift of the storm tracks[42] increases precipitation variance in some regions, exacerbating the risk of extremes, while decreasing it and alleviating the risk in other regions. On seasonal and interannual timescales, the robust projection of increased extreme El Niño frequency[53] would alter extreme precipitation patterns linked to El Niño.

Tropical cyclones (TCs) are among the most destructive storms. Some key TC statistics, such as count and track density, are tied to large-scale environmental factors like SST and vertical shear. Atmospheric models of resolution finer than 100 km show remarkable skill in capturing this environmental control and simulating spatial and temporal variability of TCs[60]. In a warmer climate, global TC counts tend to decrease in GCMs, but intense storms may become more frequent, and TC rainfall likely will intensify[14,61]. Studies projecting TC counts for individual basins show large variability, with SST change relative to the tropical mean warming accounting for much of this variability[62,63]. Because of the interhemispheric gradient in the SST increase, the TC count decrease is more pronounced in the Southern Hemisphere. The western Pacific is an exception because of strong remote SST effects, similar to what is found for ENSO-induced variability in TC genesis[63]. Mid-tropospheric vertical velocity appears to be a robust predictor of basin count change, and is tied to the distribution of SST

change. In addition to TC genesis, atmospheric circulation change impacts TC tracks, affecting statistics of TC landfall[64].

3. Challenges

For global-mean temperature projections, aerosol effects and cloud response are leading sources of uncertainty in radiative forcing and climate feedback, respectively[2]. For regional precipitation projections, we have shown that atmospheric circulation change is the major uncertainty source (Fig. S1). In the tropics, the circulation is coupled with patterns of SST change while in the extratropics, internal variability, random but organized into large-scale spatial patterns, exacerbates the circulation uncertainty.

The problem of regional climate change projections presents a range of challenges in terms of physical understanding, the observational record, climate models and the simulations we perform with them. For example, what are the long-term observational trends, and what are their causes? How sensitive are regional climate change patterns to forcing types with different spatial distributions (GHGs vs. aerosols)? How can we predict robust patterns of circulation and precipitation change? How do systematic errors in models impact the change patterns? What are the relative roles of internal variability and forced response? These questions pose new problems of ocean-atmosphere-land interactions. Understanding these interactions will allow us to reduce circulation uncertainty and build confidence in regional climate projections.

3.1 Observations

The quality of the observational record is an inherent uncertainty source, particularly pertaining to variability on decadal and longer time scales.. Limited duration, incomplete spatial coverage, and observational errors hinder our ability to characterize past changes and attribute them to anthropogenic forcing, and limit our ability to evaluate models[65].

The tropical Pacific provides an example. Observational datasets disagree on the pattern of tropical Indo-Pacific SST change[30,66]. Spatial variations in SST trends (0.2^{o}C/century) are generally smaller than the global SST increase (0.6^{o}C/century), approaching observational errors and/or internal variability. These spatial patterns drive atmospheric circulation changes, which in turn determine rainfall change patterns (sections 2.2-2.3). Since all datasets are imperfect, seeking physical consistency among observations, e.g., between the tropical SST

gradient and trade winds[67], is a way to infer regional change patterns. Model-data assimilation seeks such consistency, and proves effective for studying variability on synoptic to decadal timescales. Reanalysis products, however, often are not appropriate for climate change studies[67], as the quality and quantity of assimilated data change over time. A new generation of reanalysis suitable for climate change research is necessary, with use of coupled assimilation to improve consistency between ocean and atmospheric data.

Knowledge of the strengths and limitations of observational data sets is imperative for understanding past climate change, model evaluation, and constraining projections. Community efforts to gather such knowledge from experienced data users and developers, and to share it with the wider climate community via "open source" platforms (e.g., https://climatedataguide.ucar.edu/) are essential[68]. To facilitate multi-model assessments, open source climate model assessment packages can be valuable resources. For example, the "Climate Variability Diagnostics Package" (http://www2.cesm.ucar.edu/working-groups/cvcwg/cvdp) provides key metrics of internal climate variability across models, with comparison to observations[69]. Ongoing efforts to produce a meaningful set of metrics on mean states, internal variability, and response to external forcing are integral to advancing regional scale model evaluation (http://www-metrics-panel.llnl.gov/wiki/FrontPage). The challenge is to convert insights from model evaluation to model improvements.

3.2 Impact of model errors on projections

Despite limitations of observational records, model biases are clearly evident, reducing confidence in regional projections. A common problem is excessive summertime drying of soils in continental interiors, which may impact the land-sea warming ratio. Models simulating excessive summer Arctic sea-ice may have too weak polar amplification[70]. In the tropics, convection and rainfall are organized into east-west elongated bands called the intertropical convergence zone (ITCZ). A long-standing bias is the so-called 'double' ITCZ referring to models' failure to keep the ITCZ north of the equator over the eastern Pacific and Atlantic. The double ITCZ bias is related to atmosphere-ocean coupling errors and is likely to affect rainfall change projections in the South Pacific Islands[71] and elsewhere. The 30-60 days Madden Julian Oscillation is another phenomenon poorly represented in many models[72] affecting confidence in projections of the South Asian Monsoon, especially the subseasonal variability such as

active/break cycles. Thus, despite a relatively robust understanding of tropical rainfall changes (see section 2), the precise pattern in any particular model may not be credible.

Some biases persist over multiple model generations. It is important to move beyond routine model evaluation (e.g., root mean square errors) and develop innovative techniques to evaluate processes impacting regional projections. The equatorial Pacific cold tongue, for example, results from interaction of trade winds and ocean upwelling (Bjerknes feedback). The cold tongue extends too far west in most models, skewing ENSO SST anomaly patterns and hence atmospheric teleconnections. The balance between the Bjerknes feedback and damping by upwelling and surface heat fluxes determines the magnitude and pattern of SST response to global warming[16,18]. This balance varies considerably among models. Most CMIP5 models project larger warming in the eastern than western equatorial Pacific[14]. However, if the upwelling damping were stronger, this change in east-west gradient could reverse[73], impacting ENSO's magnitude and spatial pattern[49]. Model evaluation should quantify these ocean-atmospheric feedbacks and their role in determining the spatial pattern of SST change. Such process-based model evaluation challenges the observational record, as estimates of process-level variables may only be available from field campaigns in sparse regions and times.

A further challenge is that model processes often involve complex interactions between resolved dynamics and multiple parameterization schemes. It is not the best strategy to update parameterization schemes in isolation, since physical consistency of multiple processes is required. The 'assembly' stage of model development, often erroneously called 'model tuning', would benefit from tighter integration with process-based model evaluation. For example, long-standing tropical biases like the double ITCZ may be influenced by extratropical errors, such as Southern Ocean clouds[74] and the Atlantic meridional overturning circulation[75].

Statistical methods have been suggested to adjust regional projections based on evaluation of model errors. Bayesian techniques employ large model ensembles with perturbed parameters and weight each member according to its ability to reproduce observations[76,77]. Such approaches take into account uncertainties from multiple sources: models, observations and physical understanding. This allows us to move beyond simple ensemble mean and standard deviation approaches common in regional assessments (Fig. 1). The concept of 'emergent constraints' derives relationships between observable quantities and future projection variables in multi-model ensembles and uses the relationship to re-weight the multi-model projections in

a similar way to the Bayesian approach[70,78]. Emergent constraints cannot deal with errors common to all models, highlighting the need for innovative complementary approaches to improving models.

3.3 Effects of internal variability

Any individual observed or simulated climate trajectory contains contributions from internal variability and external forcing. The relative importance of these two contributions depends on temporal and spatial scale, and on the variable of interest[3,79,80]. In the extratropics, internal variability plays a dominant role in multidecadal atmospheric circulation changes, shaping regional patterns of temperature and precipitation changes[80]. For example, large uncertainties in North American air temperature and precipitation trends projected over the next 50 years stem mostly from internal circulation variability[81]. To the extent this internal variability is unpredictable, the resultant uncertainty is irreducible. This "single realization effect" is large enough to mask the forced regional response, presenting a major challenge for understanding and communication of regional climate change[45,82].

Due to internal variability, ensemble-mean regional climate trends may be misleading[83,84]. The top panels of Fig. 4 provide an example of a probabilistic representation of winter SAT trends at a grid point near Vienna, Austria, based on a 30-member initial condition ensemble[81]. The trend distribution is broad for 1976-2005; even with the forced response of 0.2^{o}/decade, there is a 20% chance the 30-year SAT trend is negative. As trend length increases, the radiatively forced trend increases while the trend distribution narrows, indicating reduced importance of internal variability.

Internal variability has a particularly important impact on projected changes in extreme events, as illustrated in the bottom panels of Fig. 4 for summertime temperature at the same grid box from the 30-member ensemble. Trend uncertainty over the 2001-2030 period results in substantial divergence among summertime temperature distributions (Fig. 4c), with dramatic increases in hot extremes for some realizations (e.g., realization 2) but modest increases in other realizations (e.g., realization 1). Variance changes, depicted by changes in the width of the distributions, are modest in this example. However, uncertainty in temperature trend owing to decadal internal variability broadens the ensemble's probability distribution function (Fig. 4d). This broadening indicates that internal variability averages out across realizations in

climate means, but not in extremes. Thus decadal internal variability increases the probability of extreme events by widening the tails of distribution. When coupled with potential socio-economic consequences, this would result in increase of disaster risk. While Nature makes only one realization, risk assessment (e.g., for insurance) must consider all possible outcomes based on large initial-condition ensembles from different models under a variety of forcing scenarios.

Changes in variance and skewness are also important for extreme events. The summertime temperature variance at the central European location in Fig. 4 increases by about 7% between 2001-2015 and 2016-2030, consistent with the projected increase in European summertime temperature variability[56] and contributing to widening of the probability distribution. There is evidence GCMs have considerable errors in their simulation of internal variability[3,85,86], but such evaluations are limited by an observational record that is too short to be representative of the true range of decadal variability[87]. This verification challenge is even greater for extreme events. Such events are rare by definition and therefore are even more affected by the observational record's limitations[55]. Climate model improvements, increased understanding of radiatively forced dynamical changes, and large-ensemble simulations are required to alleviate the statistical limitations of small sample sizes in a single realization.

4. Recommendations for research

We have identified key physical mechanisms for regional climate change (Fig. 5). The thermodynamic response to radiative forcing is best-understood and most robust across models. Examples include enhanced continental warming, polar amplification and the wet-gets-wetter effect. Decomposition of rainfall change into thermodynamic and dynamic components shows that atmospheric circulation change is the main source of uncertainty in regional projections. Understanding the mechanisms for circulation change is essential to reduce this uncertainty, but they have only begun to be explored. More research is needed on how aerosol forcing can induce regional atmospheric circulation change (e.g., the Asian summer monsoon). Recent studies suggest that despite large uncertainties in aerosol radiative forcing, there are robust planetary-scale response patterns, mediated by ocean coupling.

Our review suggests distinct regimes of atmospheric circulation change in the tropics versus the mid-latitudes, calling for different approaches. In the tropics, internal variability on decadal time scales and longer is relatively small in comparison to the forced signal on the

centennial horizon, and models now agree on some aspects of the pattern of rainfall change that are projected to emerge by the end of this century (e.g., an increase in the equatorial Pacific and Atlantic, and a decrease in the southeastern tropical oceans). Precipitation and atmospheric circulation are tightly coupled with the SST change pattern in both the multi-model mean projection and inter-model variability. Elucidating this coupling, and developing observational constraints, can narrow uncertainties of regional projections in the tropics. An analog may be the historical development of ENSO prediction, where theory initially explained how coupled modes emerge from ocean-atmosphere feedback, ultimately laying the foundation for seasonal climate prediction. The challenge is to extend this success to radiatively forced problems, and to design observing systems that monitor key processes associated with ongoing climate change.

In the midlatitudes, by contrast, coupling between large-scale atmospheric circulation and local SSTs is weak. Internal variability plays a much larger role in generating differences among regional-scale projections. Nevertheless, the lack of a robust circulation response in midlatitudes in models does not preclude potential shifts in storm tracks or changes in blocking frequency that models cannot, yet, represent. Random internal variability and the non-linear nature of the midlatitude circulation render regional climate projections inherently probabilistic.

We recommend a coordinated multi-model set of large initial-condition ensembles to further regional climate change research (Box 1). First, such a set of experiments would quantify probabilities of changes in means and extremes across models, including not only structural uncertainty but also irreducible uncertainty due to internal variability. Quantification of changes in risks is necessary for insurance, and infrastructure planning. To quantify probability distributions and occurrence of extremes, we need research into dynamical processes governing changes in higher-order moments such as variance and skewness. Second, the set of experiments would enable isolation of uncertainties due to internal variability from those due to model structure. Large ensembles also open new possibilities to study radiatively-forced changes in extratropical atmospheric circulation.

Computing advances have benefited climate modeling through enhanced complexity and increased resolution. A threshold has recently been crossed: at 50 km resolution, atmospheric models demonstrate marked skill in simulating TC statistics. This opens up new opportunities for studying climate change effects on TC variability, much like the 1970s-80s, when explicit simulations of extratropical cyclones dramatically improved weather forecasts.

High-resolution large-ensemble simulations could greatly advance our understanding of internal variability and forced change in TC metrics and processes, especially track density, landfall statistics and ocean feedback. Higher resolution also improves simulation of blocking events, a phenomenon linked to extreme weather in the extratropics.

Robust precipitation changes are projected over land: increases at high latitudes and in the Asian monsoon result from enhanced atmospheric moisture content, while decreases in the subtropics arise from Hadley cell expansion. The ocean warming pattern also changes atmospheric circulation over the Sahel and Amazon, although the robustness of these changes remains to be tested. In addition to such non-local atmospheric changes, improved understanding of land surface processes is key to more credible projections of human impacts[58,88]. For example, soil moisture and near-surface relative humidity are projected to decrease globally[89], likely exacerbating drought when it does occur, and potentially increasing heat wave frequency and intensity. More realistic simulation of snow albedo feedback and snow processes would also reduce uncertainty surrounding continental warming, runoff timing, and soil moisture at high latitudes[90].

Agreement among models is an indicator of robust change, but should be viewed in the context of model biases and weak observational constraints on forced regional response. Evaluating the impact of common biases and ultimately reducing them is a grand challenge. The daily verification cycle has enabled weather forecasts to improve steadily by exposing model errors and observational needs. Similarly, seasonal prediction[91] and attribution studies of extreme climate events[92] can improve physical understanding and build model confidence. In this context, pacemaker experiments—partial coupling that prescribes observed SST or wind evolution in tropical oceans[19,93,94]—are useful to identify key drivers of regional change. Further innovations in experimental design are necessary to expose model problems. For example, flux-adjusted models can be run in parallel with freely-evolving models to evaluate effects of model biases on regional projections.

Regional climate projections are often taken as synonymous with downscaling global scenarios. The misconception is that with enhanced resolution, regional models will automatically solve the problem of producing regional climate projections. Downscaling global model projections without carefully considering model biases and internal variability adds essentially meaningless spatial detail[1]. Regional models may be useful to understand physical

processes in areas of complex coastlines and orography, and may provide useful climate change impact information on the km scales relevant to climate adaptation planning[95]. We suggest, however, that the current priority is to understand and reduce GCM uncertainties on regional scales (> 100 km), which often dictate changes on finer-scales. To achieve reliable regional climate projections, it is essential to understand the underlying physics, reduce model biases, and adequately account for internal variability.

Box 1. Modeling strategies

With limited computational resources, it is critical to make optimal use of computing resources to advance regional climate change projections, and to correctly assess uncertainties, reducing them when possible.

There are a number of demands on computer and human resources (Fig. 6). A variety of independent models, differing significantly in their underlying physics and numerics, are required to provide assessments of the range of possible climate change. Models are also being developed that contain ever more complete representations of the climate system, including processes such as biogeochemical cycles, atmospheric chemistry and aerosols, clouds and convection, land processes and ice sheets. Process-oriented experiments are needed to better understand model behaviour, including internal variability and the response to various radiative forcing. The following factors increase demands on computational resources: First, internal variability has a very strong imprint on climate trends even on time scales as long as several decades and spatial scales as large as continents[81]. This calls for large ensemble simulations[96]. Second, when spatial resolution is high (25-50 km), many phenomena are reasonably well simulated in GCMs[97], including tropical cyclones[63,91] and extratropical weather regimes such as blocking[98,99]. This makes higher resolution desirable.

Regional models are useful to understand the role of small-scale processes in shaping the regional climate response. These processes include orographic precipitation, snow-albedo feedback, land-sea breeze circulation systems, mesoscale convective systems, and ocean feedbacks on tropical cyclone intensity. Orography and coastline geography unresolved by global models can introduce credibility into regional patterns obtained with downscaling techniques Such smaller-scale mechanisms need to be carefully evaluated to establish credibility[100].

We recommend the following modeling strategies to achieve more reliable regional climate projections. These recommendations contribute to the ongoing planning for the next phase of CMIP and grand challenges of the World Climate Research Programme.

- To develop innovative experiments to shed light on atmospheric circulation response to radiative forcing, and to explore the sensitivity to ocean coupling, land surface processes and other important physical processes such as convection;
- To perform large ensemble simulations to isolate forced change and internal variability, and estimate the probability distribution of regional change;
- To exploit the emerging capability of high-resolution modeling to simulate important extreme phenomena such as tropical cyclones, and take advantage of resolved local geographical features like the coastline and orography;
- To run the models for scenario projections in initialized mode and verify their subseasonal to interannual climate predictions, and to test models' skill in simulating important climate events such as mega droughts;
- To explore model development practices that effectively incorporate insights from process-based model evaluation and integrate multiple coupled processes for overall physical consistency.

References

1 Hall, A. Projecting regional change. *Science* **346**, 1461-1462 (2014).

2 IPCC. Summary for policymakers. In: *Climate Change 2013: The Physical Science Basis.* (eds Stocker, T.F. et al.) 1-29 (Cambridge University Press, 2013).

3 Hawkins, E. & Sutton, R. The potential to narrow uncertainty in regional climate predictions. *Bull. Am. Meteorol. Soc.* **90**, 1095-1107 (2009).

4 Collins, M. *et al.* Long-term climate change: projections, commitments and irreversibility. In: *Climate Change 2013: The Physical Science Basis.* (eds Stocker, T.F. et al.) 1029-1136 (Cambridge University Press, 2013).

5 Webb, M. J., Lambert, F. H. & Gregory, J. M. Origins of differences in climate sensitivity, forcing and feedback in climate models. *Clim. Dyn.* **40**, 677-707 (2013).

6 Pithan, F. & Mauritsen, T. Arctic amplification dominated by temperature feedbacks in contemporary climate models. *Nature Geosci.* **7**, 181-184 (2014).

7 Screen, J. A. & Simmonds, I. The central role of diminishing sea ice in recent Arctic temperature amplification. *Nature* **464**, 1334-1337 (2010).

8 Joshi, M. M., Turner, A. G. & Hope, C. The use of the land-sea warming contrast under climate change to improve impact metrics. *Clim. Change* **117**, 951-960 (2013).

9 Manabe, S. & Stouffer, R. J. Role of ocean in global warming. *J. Meteorol. Soc. Jpn.* **85B**, 385-403 (2007).

10 Marshall, J. *et al.* The ocean's role in polar climate change: Asymmetric Arctic and Antarctic responses to greenhouse gas and ozone forcing. *Philos. T. R. Soc. A.* **372** (2014).

11 Harris, G. R., Sexton, D. M. H., Booth, B. B. B., Collins, M. & Murphy, J. M. Probabilistic projections of transient climate change. *Clim. Dyn.* **40**, 2937-2972 (2013).

12 Chou, C. & Neelin, J. D. Mechanisms of global warming impacts on regional tropical precipitation. *J. Clim.* **17**, 2688-2701 (2004).

13 Held, I. M. & Soden, B. J. Robust responses of the hydrological cycle to global warming. *J. Clim.* **19**, 5686-5699 (2006).

14 Christensen, J. H. *et al.* Climate phenomena and their relevance for future regional climate change. In: *Climate Change 2013: The Physical Science Basis.* (eds Stocker, T.F. et al.) 1217-1308 (Cambridge University Press, 2013).

15 Seager, R., Naik, N. & Vecchi, G. A. Thermodynamic and dynamic mechanisms for large-scale changes in the hydrological cycle in response to global warming. *J. Clim.* **23**, 4651-4668 (2010).

16 Xie, S. P. *et al.* Global warming pattern formation: Sea surface temperature and rainfall. *J. Clim.* **23**, 966-986 (2010).

17 Widlansky, M. J. *et al.* Changes in South Pacific rainfall bands in a warming climate. *Nature Clim. Change* **3**, 417-423 (2013).

18 Liu, Z. Y., Vavrus, S., He, F., Wen, N. & Zhong, Y. F. Rethinking tropical ocean response to global warming: The enhanced equatorial warming. *J. Clim.* **18**, 4684-4700 (2005).

19 Kosaka, Y. & Xie, S. P. Recent global-warming hiatus tied to equatorial Pacific surface cooling. *Nature* **501**, 403-407 (2013).

20 Chadwick, R., Boutle, I. & Martin, G. Spatial patterns of precipitation change in CMIP5: why the rich do not get richer in the tropics. *J. Clim.* **26**, 3803-3822 (2013).

21 Huang, P., Xie, S. P., Hu, K. M., Huang, G. & Huang, R. H. Patterns of the seasonal response of tropical rainfall to global warming. *Nature Geosci.* **6**, 357-361 (2013).

22 Biasutti, M. & Sobel, A. H. Delayed Sahel rainfall and global seasonal cycle in a warmer climate. *Geophys. Res. Lett.* **36**, L23707 (2009).
23 Neelin, J. D., Chou, C. & Su, H. Tropical drought regions in global warming and El Nino teleconnections. *Geophys. Res. Lett.* **30**, 2275 (2003).
24 Seth, A. *et al.* CMIP5 projected changes in the annual cycle of precipitation in monsoon regions. *J. Clim.* **26**, 7328-7351 (2013).
25 Anderson, B. T. *et al.* Sensitivity of terrestrial precipitation trends to the structural evolution of sea surface temperatures. *Geophys. Res. Lett.* **42**, 1190-1196 (2015).
26 Giannini, A. *et al.* A unifying view of climate change in the Sahel linking intra-seasonal, interannual and longer time scales. *Environ. Res. Lett.* **8**, 024010 (2013).
27 Ma, J. & Xie, S.-P. Regional patterns of sea surface temperature change: A source of uncertainty in future projections of precipitation and atmospheric circulation. *J. Clim.* **26**, 2482-2501 (2013).
28 Li, W. H., Fu, R. & Dickinson, R. E. Rainfall and its seasonality over the Amazon in the 21st century as assessed by the coupled models for the IPCC AR4. *J. Geophys. Res.-Atmos.* **111**, D02111 (2006).
29 Harris, P. P., Huntingford, C. & Cox, P. M. Amazon Basin climate under global warming: The role of the sea surface temperature. *Philos. T. R. Soc. B.* **363**, 1753-1759 (2008).
30 Vecchi, G. A. & Soden, B. J. Global warming and the weakening of the tropical circulation. *J. Clim.* **20**, 4316-4340 (2007).
31 Lu, J., Vecchi, G. A. & Reichler, T. Expansion of the Hadley cell under global warming. *Geophys. Res. Lett.* **34**, L06805 (2007).
32 Scheff, J. & Frierson, D. Twenty-first-century multimodel subtropical precipitation declines are mostly midlatitude shifts. *J. Clim.* **25**, 4330-4347 (2012).
33 Delworth, T. L. & Zeng, F. R. Regional rainfall decline in Australia attributed to anthropogenic greenhouse gases and ozone levels Latitude. *Nature Geosci.* **7**, 583-587 (2014).
34 Li, W. H., Li, L. F., Ting, M. F. & Liu, Y. M. Intensification of Northern Hemisphere subtropical highs in a warming climate. *Nature Geosci.* **5**, 830-834 (2012).
35 Shindell, D. T., Voulgarakis, A., Faluvegi, G. & Milly, G. Precipitation response to regional radiative forcing. *Atmos. Chem. Phys.* **12**, 6969-6982 (2012).
36 Ming, Y. & Ramaswamy, V. A model investigation of aerosol-induced changes in tropical circulation. *J. Clim.* **24**, 5125-5133 (2011).
37 Rotstayn, L. D. & Lohmann, U. Tropical rainfall trends and the indirect aerosol effect. *J. Clim.* **15**, 2103-2116 (2002).
38 Chang, C. Y., Chiang, J. C. H., Wehner, M. F., Friedman, A. R. & Ruedy, R. Sulfate aerosol control of tropical Atlantic climate over the twentieth century. *J. Clim.* **24**, 2540-2555 (2011).
39 Li, X., Ting, M., Li, C. & Henderson, N. Mechanisms of Asian Summer Monsoon changes in response to anthropogenic forcing in CMIP5 models. *J. Clim.* in press, doi: http://dx.doi.org/10.1175/JCLI-D-14-00559.1 (2015).
40 Xie, S. P., Lu, B. & Xiang, B. Q. Similar spatial patterns of climate responses to aerosol and greenhouse gas changes. *Nature Geosci.* **6**, 828-832 (2013).
41 Rosenfeld, D., Sherwood, S., Wood, R. & Donner, L. Climate effects of aerosol-cloud interactions. *Science* **343**, 379-380 (2014).

42 Yin, J. H. A consistent poleward shift of the storm tracks in simulations of 21st century climate. *Geophys. Res. Lett.* **32**, L18701 (2005).
43 Barnes, E. A. & Polvani, L. Response of the midlatitude jets, and of their variability, to increased greenhouse gases in the CMIP5 models. *J. Clim.* **26**, 7117-7135 (2013).
44 Kang, S. M., Polvani, L. M., Fyfe, J. C. & Sigmond, M. Impact of polar ozone depletion on subtropical precipitation. *Science* **332**, 951-954 (2011).
45 Shepherd, T. G. Atmospheric circulation as a source of uncertainty in climate change projections. *Nature Geosci.* **7**, 703-708 (2014).
46 van Oldenborgh, G. J., Philip, S. Y. & Collins, M. El Nino in a changing climate: a multi-model study. *Ocean. Sci.* **1**, 81-95 (2005).
47 Watanabe, M. *et al.* Uncertainty in the ENSO amplitude change from the past to the future. *Geophys. Res. Lett.* **39**, L20703 (2012).
48 Bellenger, H., Guilyardi, E., Leloup, J., Lengaigne, M. & Vialard, J. ENSO representation in climate models: From CMIP3 to CMIP5. *Clim. Dyn.* **42**, 1999-2018 (2014).
49 Collins, M. *et al.* The impact of global warming on the tropical Pacific ocean and El Nino. *Nature Geosci.* **3**, 391-397 (2010).
50 DiNezio, P. N. *et al.* Mean climate controls on the simulated response of ENSO to increasing greenhouse gases. *J. Clim.* **25**, 7399-7420 (2012).
51 Wittenberg, A. T. Are historical records sufficient to constrain ENSO simulations? *Geophys. Res. Lett.* **36**, L12702 (2009).
52 Power, S., Delage, F., Chung, C., Kociuba, G. & Keay, K. Robust twenty-first-century projections of El Nino and related precipitation variability. *Nature* **502**, 541-545 (2013).
53 Cai, W. J. *et al.* Increasing frequency of extreme El Nino events due to greenhouse warming. *Nature Clim. Change* **4**, 111-116 (2014).
54 Griffiths, G. M. *et al.* Change in mean temperature as a predictor of extreme temperature change in the Asia-Pacific region. *Int. J. Climatol.* **25**, 1301-1330 (2005).
55 Seneviratne, S. I. *et al.* Changes in climate extremes and their impacts on the natural physical environment. In: *Managing the Risks of Extreme Events and Disasters to Advance Climate Change Adaptation*. (eds Field, C.B. et al.) 109-230 (Cambridge University Press, 2013).
56 Huntingford, C., Jones, P. D., Livina, V. N., Lenton, T. M. & Cox, P. M. No increase in global temperature variability despite changing regional patterns. *Nature* **500**, 327-330 (2013).
57 Screen, J. A. Arctic amplification decreases temperature variance in northern mid- to high-latitudes. *Nature Clim. Change* **4**, 577-582 (2014).
58 Seneviratne, S. I., Luthi, D., Litschi, M. & Schar, C. Land-atmosphere coupling and climate change in Europe. *Nature* **443**, 205-209 (2006).
59 Meehl, G. A., Arblaster, J. M. & Tebaldi, C. Understanding future patterns of increased precipitation intensity in climate model simulations. *Geophys. Res. Lett.* **32**, L18719 (2005).
60 Walsh, K. J. E. *et al.* Hurricanes and climate: The U.S. CLIVAR working group on hurricanes. *Bull. Am. Meteorol. Soc.*, in press, doi:10.1175/bams-d-13-00242.1 (2015).
61 Knutson, T. R. *et al.* Tropical cyclones and climate change. *Nature Geosci.* **3**, 157-163 (2010).
62 Vecchi, G. A., Swanson, K. L. & Soden, B. J. Climate change whither hurricane activity? *Science* **322**, 687-689 (2008).

63 Zhao, M. & Held, I. M. TC-permitting GCM simulations of hurricane frequency response to sea surface temperature anomalies projected for the late-twenty-first century. *J. Clim.* **25**, 2995-3009 (2012).
64 Murakami, H., Wang, B., Li, T. & Kitoh, A. Projected increase in tropical cyclones near Hawaii. *Nature Clim. Change* **3**, 749-754 (2013).
65 Goddard, L. *et al.* A verification framework for interannual-to-decadal predictions experiments. *Clim. Dyn.* **40**, 245-272 (2013).
66 Deser, C., Phillips, A. S. & Alexander, M. A. Twentieth century tropical sea surface temperature trends revisited. *Geophys. Res. Lett.* **37**, L10701 (2010).
67 Tokinaga, H., Xie, S. P., Deser, C., Kosaka, Y. & Okumura, Y. M. Slowdown of the Walker circulation driven by tropical Indo-Pacific warming. *Nature* **491**, 439-443 (2012).
68 Schneider, D. P., Deser, C., Fasullo, J. & Trenberth, K. E. Climate data guide spurs discovery and understanding. *EOS, Trans. Amer. Geophys. Union* **94**, 121-122 (2013).
69 Phillips, A. S., Deser, C. & Fasullo, J. The NCAR climate variability diagnostics package with relevance to model evaluation. *EOS, Trans. Amer. Geophys. Union* **95**, 453-455 (2014).
70 Bracegirdle, T. J. & Stephenson, D. B. On the robustness of emergent constraints used in multimodel climate change projections of Arctic warming. *J. Clim.* **26**, 669-678 (2013).
71 Brown, J. N. *et al.* Implications of CMIP3 model biases and uncertainties for climate projections in the western tropical Pacific. *Clim. Change* **119**, 147-161 (2013).
72 Hung, M. P. *et al.* MJO and convectively coupled equatorial waves simulated by CMIP5 climate models. *J. Clim.* **26**, 6185-6214 (2013).
73 Clement, A. C., Seager, R., Cane, M. A. & Zebiak, S. E. An ocean dynamical thermostat. *J. Clim.* **9**, 2190-2196 (1996).
74 Hwang, Y. T. & Frierson, D. M. W. Link between the double-Intertropical Convergence Zone problem and cloud biases over the Southern Ocean. *Proc. Natl Acad. Sci. USA* **110**, 4935-4940 (2013).
75 Wang, C. Z., Zhang, L. P., Lee, S. K., Wu, L. X. & Mechoso, C. R. A global perspective on CMIP5 climate model biases. *Nature Clim. Change* **4**, 201-205 (2014).
76 Collins, M. *et al.* Quantifying future climate change. *Nature Clim. Change* **2**, 403-409 (2012).
77 Rougier, J. Probabilistic inference for future climate using an ensemble of climate model evaluations. *Clim. Change* **81**, 247-264 (2007).
78 Boe, J. L., Hall, A. & Qu, X. September sea-ice cover in the Arctic Ocean projected to vanish by 2100. *Nature Geosci.* **2**, 341-343 (2009).
79 Deser, C., Phillips, A., Bourdette, V. & Teng, H. Y. Uncertainty in climate change projections: The role of internal variability. *Clim. Dyn.* **38**, 527-546 (2012).
80 Wallace, J. M., Deser, C., Smoliak, B. V. & Phillips, A. S. Attribution of climate change in the presence of internal variability, In: *Climate Change: Multidecadal and Beyond. In World Scientific Series on Asia-Pacific Weather and Climate Vol. 6* (eds Chang, C. P. et al.) in press (2015).
81 Deser, C., Phillips, A. S., Alexander, M. A. & Smoliak, B. V. Projecting North American climate over the next 50 years: Uncertainty due to internal variability. *J. Clim.* **27**, 2271-2296 (2014).
82 Ricke, K. L. & Caldeira, K. Natural climate variability and future climate policy. *Nature Clim. Change* **4**, 333-338 (2014).

83 Raisanen, J. & Palmer, T. N. A probability and decision-model analysis of a multimodel ensemble of climate change simulations. *J. Clim.* **14**, 3212-3226 (2001).
84 Tebaldi, C. & Knutti, R. The use of the multi-model ensemble in probabilistic climate projections. *Philos. T. R. Soc. A.* **365**, 2053-2075 (2007).
85 van Oldenborgh, G. J., Reyes, F. J. D., Drijfhout, S. S. & Hawkins, E. Reliability of regional climate model trends. *Environ. Res. Lett.* **8**, 014055 (2013).
86 Yokohata, T. *et al.* Reliability of multi-model and structurally different single-model ensembles. *Clim. Dyn.* **39**, 599-616 (2012).
87 Partin, J. W. *et al.* Multidecadal rainfall variability in South Pacific Convergence Zone as revealed by stalagmite geochemistry. *Geology* **41**, 1143-1146 (2013).
88 Dirmeyer, P. A., Jin, Y., Singh, B. & Yan, X. Q. Trends in Land-Atmosphere Interactions from CMIP5 Simulations. *J. Hydro.* **14**, 829-849 (2013).
89 Sherwood, S. & Fu, Q. A drier future? *Science* **343**, 737-739 (2014).
90 Hall, A., Qu, X. & Neelin, J. D. Improving predictions of summer climate change in the United States. *Geophys. Res. Lett.* **35**, L01702 (2008).
91 Vecchi, G. A. *et al.* On the seasonal forecasting to regional tropical cyclone activity. *J. Clim.* **27**, 7994-8016 (2014).
92 Peterson, T. C. *et al.* Explaining extreme events of 2011 from a climate perspective. *Bull. Am. Meteorol. Soc.* **93**, 1041-1067 (2012).
93 Zhang, R. & Delworth, T. L. Impact of Atlantic multidecadal oscillations on India/Sahel rainfall and Atlantic hurricanes. *Geophys. Res. Lett.* **33**, L17712 (2006).
94 England, M. H. *et al.* Recent intensification of wind-driven circulation in the Pacific and the ongoing warming hiatus. *Nature Clim. Change* **4**, 222-227 (2014).
95 Walton, D., Sun, F., Hall, A. & Capps, S. C. A hybrid dynamical–statistical downscaling technique, part I: Development and validation of the technique. *J. Clim.* in press, doi: http://dx.doi.org/10.1175/JCLI-D-14-00196.1 (2015).
96 Taschetto, A. S. & England, M. H. Estimating ensemble size requirements of AGCM simulations. *Meteorol Atmos Phys* **100**, 23-36 (2008).
97 Delworth, T. L. *et al.* Simulated climate and climate change in the GFDL CM2.5 high-resolution coupled climate model. *J. Clim.* **25**, 2755-2781 (2012).
98 Berckmans, J., Woollings, T., Demory, M. E., Vidale, P. L. & Roberts, M. Atmospheric blocking in a high resolution climate model: Influences of mean state, orography and eddy forcing. *Atmos. Sci. Lett.* **14**, 34-40 (2013).
99 Dawson, A. & Palmer, T. Simulating weather regimes: Impact of model resolution and stochastic parameterization. *Clim. Dyn.*, **44**, 2177-2193 (2015).
100 Leung, L. R. *et al.* Mid-century ensemble regional climate change scenarios for the western United States. *Clim. Change* **62**, 75-113 (2004).

Acknowledgements S.M. Long drew Figs. 2 and 3. S.P.X. is supported by National Science Foundation (NSF) and National Oceanic and Atmospheric Administration (NOAA); and M.C. by NERC NE/I022841/1. NCAR is supported by the NSF.

Author contributions
S.P.X., C.D. and M.C. led the writing of the paper. All authors contributed to the development and writing of the paper.

Additional information
Supplementary information is available in the online version of the paper. Reprints and permissions information is available online at www.nature.com/reprints. Correspondence should be addressed to S.P.X.

Competing financial interests
The authors declare no competing financial interests.

Figure captions

Figure 1 | **CMIP5 multi-model mean changes**. Surface air temperature (**a**) and precipitation (**b**) under Representative Concentration Pathway (RCP) 4.5 for the period 2081-2100 expressed as anomalies from 1986-2005, as the ensemble mean of 42 models available in CMIP5. Hatching indicates regions where the multi-model mean change is less than the natural variability (computed from 20-year averages taken from pre-industrial control experiments). Images generated using http://climexp.knmi.nl/plot_atlas_form.py.

Figure 2 | **Effect of ocean warming pattern on precipitation change**. Precipitation change (color shading, mm/month) for (**a**) spatial-uniform SST increase (SUSI) of 4K, (**b**) spatial-patterned SST increase (SPSI), and (**c**) the difference between the runs. SPSI is derived as the CMIP3 mean from the 1%/year CO2 increase runs at the time of quadrupling. All the results are scaled to a tropical (25°S-25°N) mean SST increase of 4K, based on the ensemble average of 11 atmospheric GCMs available in CMIP5. Line contours are for climatological precipitation (150, 200, 250 and 300 mm/month contours) in (**a**), and for SST deviations from the tropical mean warming (0.4 K intervals; zero contour thickened) in (**b**).

Figure 3 | **Inter-model spread of tropical precipitation change** (ΔP, mm/month). **(a)** Inter-model standard deviation of precipitation change $\sigma(\Delta P')$, along with climatological precipitation (150, 200, 250 and 300 mm/month contours). Here $\Delta P = \Delta P_{MME} + \Delta P'$, where the prime denotes the inter-model deviation from the multi-model ensemble (MME) mean. **(b)** Standard deviation of spatial variations of ΔP' within 30°S-30°N (cross marks for individual models) as a measure of uncertainty, based on 70-year trends from 1% CO2 increase to quadrupling runs with 20 CMIP5 models. ΔP is decomposed into dynamic and thermodynamic components. The open circle denotes the ensemble mean, and the error bar one standard deviation. The dynamic component is highly variable among models and the largest uncertainty of rainfall projections. $\Delta P_{dyn} = -\frac{1}{\rho_w g}\int_0^{p_s}(\Delta\omega \cdot \frac{\partial q}{\partial P})dp$, and $\Delta P_{ther} = -\frac{1}{\rho_w g}\int_0^{p_s}\left(\omega \cdot \frac{\partial \Delta q}{\partial P}\right)dp$, where p is pressure, q specific humidity, ω pressure velocity, ρ_w the density of water, g gravity, and the subscript s denotes surface value. All results are scaled to a tropical (25°S-25°N) mean SST increase of 4K in each model.

Figure 4 | **Probabilistic representation of regional climate change** at a grid box near Vienna, Austria (48.5°N, 16.2°E). (**a**) Frequency distributions, binned at intervals of 0.5°C [50 yr]$^{-1}$, of the 1976-2005 and 1976-2080 wintertime (December-February) SAT trends from a 30-member CESM ensemble under the Representative Concentration Pathway (RCP) 8.5. (**b**) The frequency of linear trend exceedance for trends that begin in 1976 and end in different years (x-axis) at the grid point. The trend threshold (filled contours at intervals of 0.25°C [50 yr]$^{-1}$) at the α frequency of exceedance is determined by the (100 - α) percentile of the 30 ensemble member trends. The plotted exceedance frequency limits are 2.5% and 97.5%. The radiatively forced trend is approximated by the median trend. (**c**) Estimates of probability distribution functions of summer (June-August) mean SAT anomalies, defined by the 1951-2000 base period. The PDF of a "typical" realization for 2001-2015 (dashed black) is determined as the normal distribution with mean and standard deviation of the 30-member ensemble. The purple and orange curves are 2016-2030 PDF estimates from two individual ensemble members, obtained by kernel density estimation. Deviations from the seasonal mean for the PDFs are obtained by subtracting the seasonal SAT anomaly from the 2001-2030 linear trend. (**d**) As in (c) but the thick red curve represents the 2016-2030 estimated PDF from the full ensemble by adopting the normal distribution with variance equal to $(\sigma_0^2 + \sigma_\mu^2)$, where σ_0 is the ensemble mean of the seasonal standard deviation from the 2016-2030 mean (0.85°C) and σ_μ is the ensemble standard deviation of the 2016-2030 mean SAT anomalies (0.23°C), indicating the widening impact of trend uncertainty on the ensemble PDF. The dashed red curve is the estimate derived directly from the histogram of the 30 ensemble members. The expected increase in hot extremes, depicted by the area in red shading, is due to both rightward shift of the PDF and the PDF broadening owing to trend uncertainty from natural variability and an increase in σ_0 from 0.80 to 0.85°C.

Figure 5 | **Schematic of physical origins of regional climate change.**

Figure 6 | Competing priorities for running climate simulations. Many choices have to be made in designing an ensemble to produce information about past and future climates. These choices include: (i) 'Variety' - the number of (pseudo-)independent simulators, (ii) 'Complexity'

- the number of physical, chemical & biological processes included in the simulator, (iii) 'Resolution' - the grid spacing, (iv) 'Experiments' - how many different types of simulation to be performed, (v) 'Domain' - whether the simulation needs to be global & coupled or regional atmosphere-only, (vi) 'Ensemble' - the number of independent realisations, (vii) 'Length' of the simulation. Different purposes and questions require different ensemble design strategies. For example, CMIP5 made a set of core choices (grey) to use many different global simulators, to typically run several different long experiments with medium complexity and resolution with small ensemble sizes. This core ensemble was designed to answer specific questions about how climate has changed in the recent past and may change in the future with different emission scenarios. Alternatively, if the question was to determine how the probabilities of certain outcomes may change in the near-term (next 20 years) on regional scales, a different design is required (orange). Or, if the focus is on detailed downscaling using regional models for future time slices then a different set of decisions would be made (green). For detection & attribution of past climatic changes, a large number of experiments are needed (blue). Note that some of these categories are serial, i.e. more time is required to complete the simulations, and some are parallel which means additional processors could be used to perform the simulations in the same time.

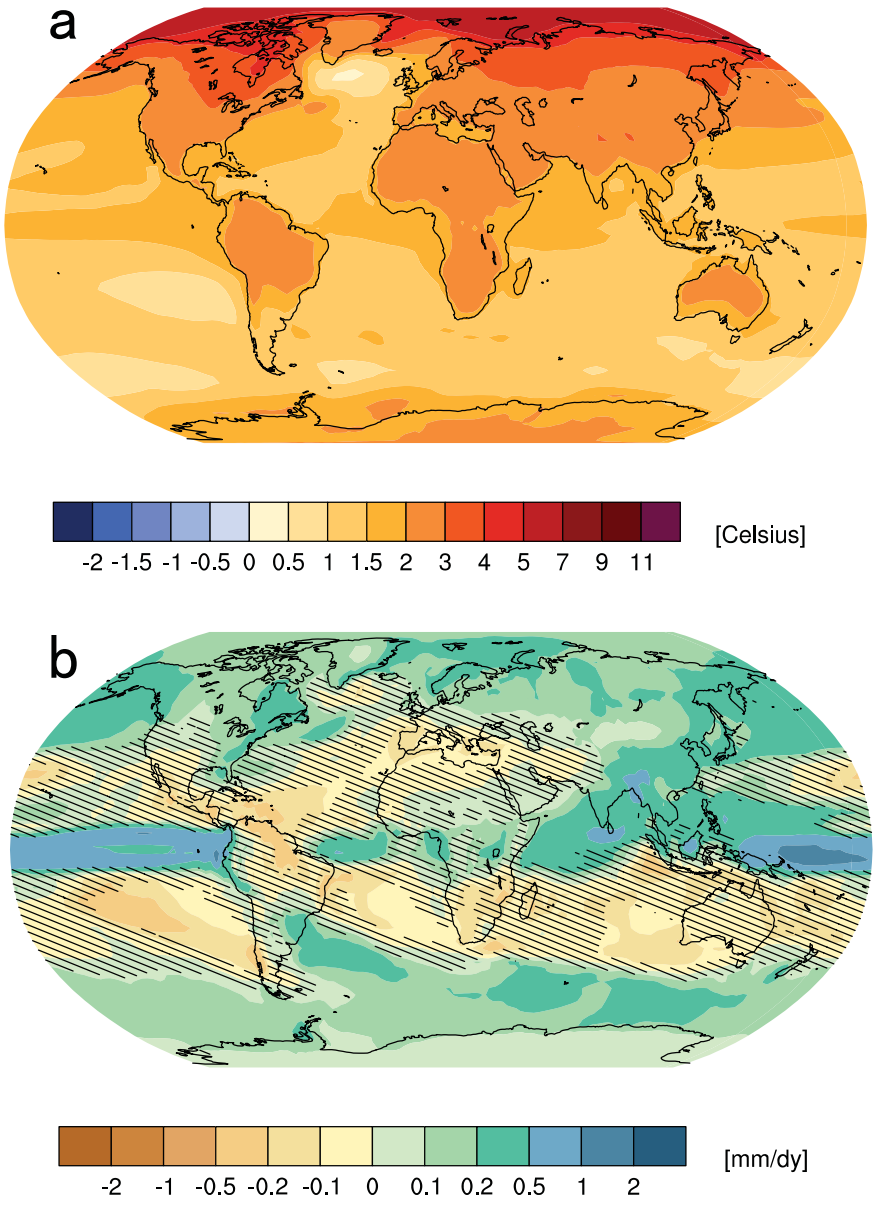
a
-2 -1.5 -1 -0.5 0 0.5 1 1.5 2 3 4 5 7 9 11
[Celsius]
b
-2 -1 -0.5 -0.2 -0.1 0 0.1 0.2 0.5 1 2
[mm/dy]

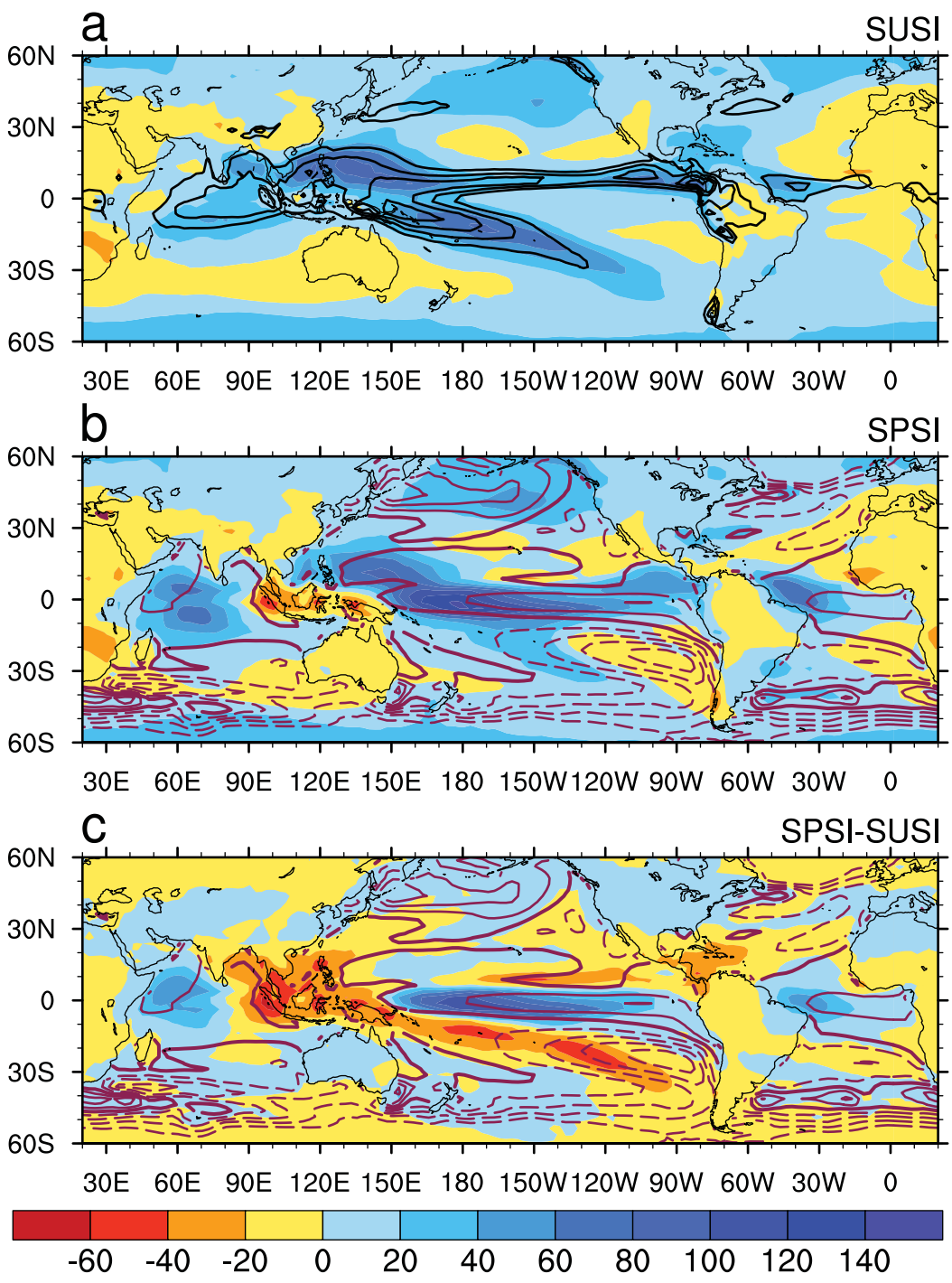
a
SUSI
60N
30N
0
30S
60S
30E 60E 90E 120E 150E 180 150W 120W 90W 60W 30W 0
b
SPSI
60N
30N
0
30S
60S
30E 60E 90E 120E 150E 180 150W 120W 90W 60W 30W 0
c
SPSI-SUSI
60N
30N
0
30S
60S
30E 60E 90E 120E 150E 180 150W 120W 90W 60W 30W 0
-60 -40 -20 0 20 40 60 80 100 120 140

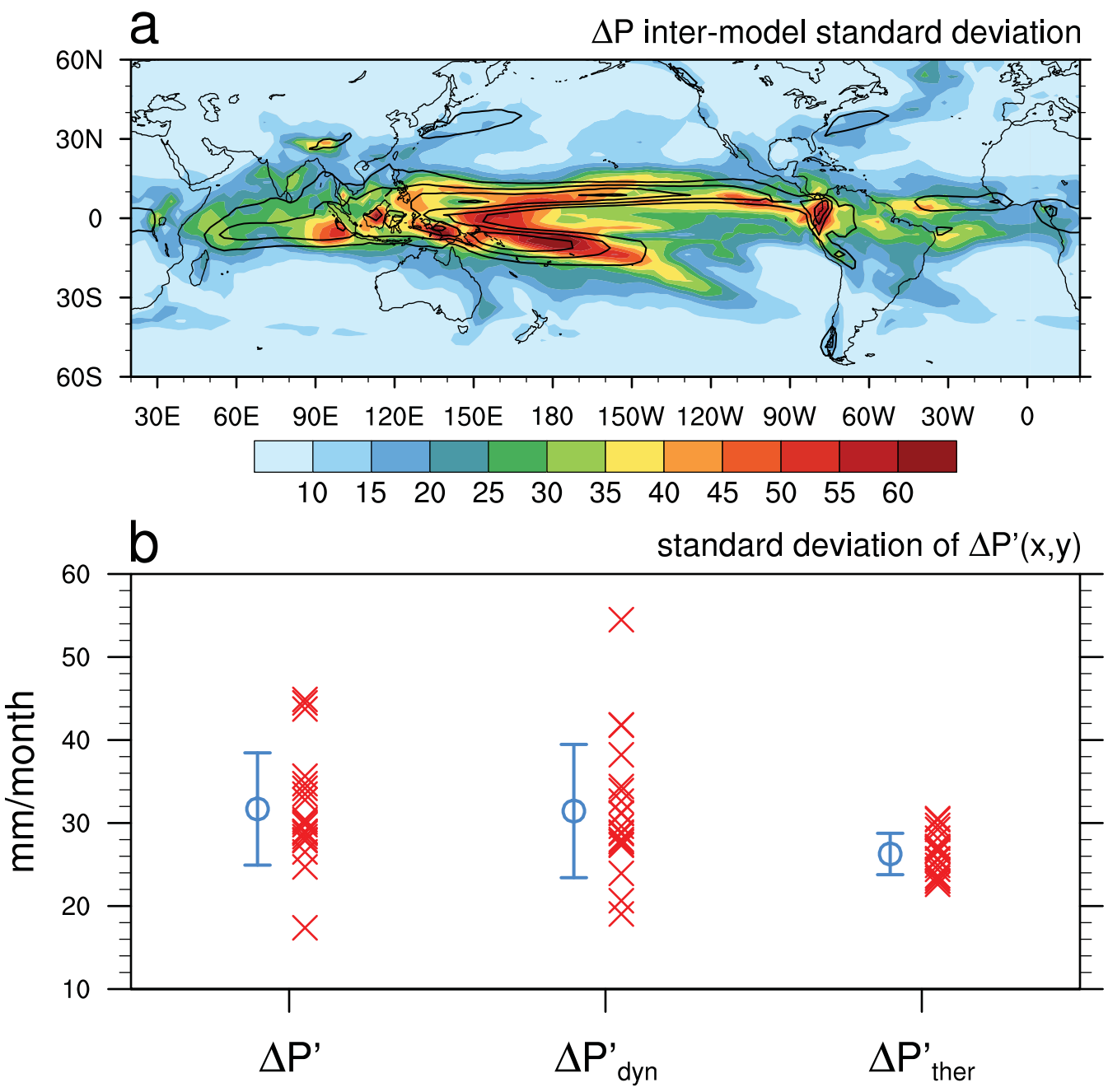
a
ΔP inter-model standard deviation
60N
30N
0
30S
60S
30E
60E
90E
120E
150E
180
150W
120W
90W
60W
30W
0
10
15
20
25
30
35
40
45
50
55
60
b
standard deviation of ΔP'(x,y)
mm/month
60
50
40
30
20
10
ΔP'
ΔP'dyn
ΔP'ther

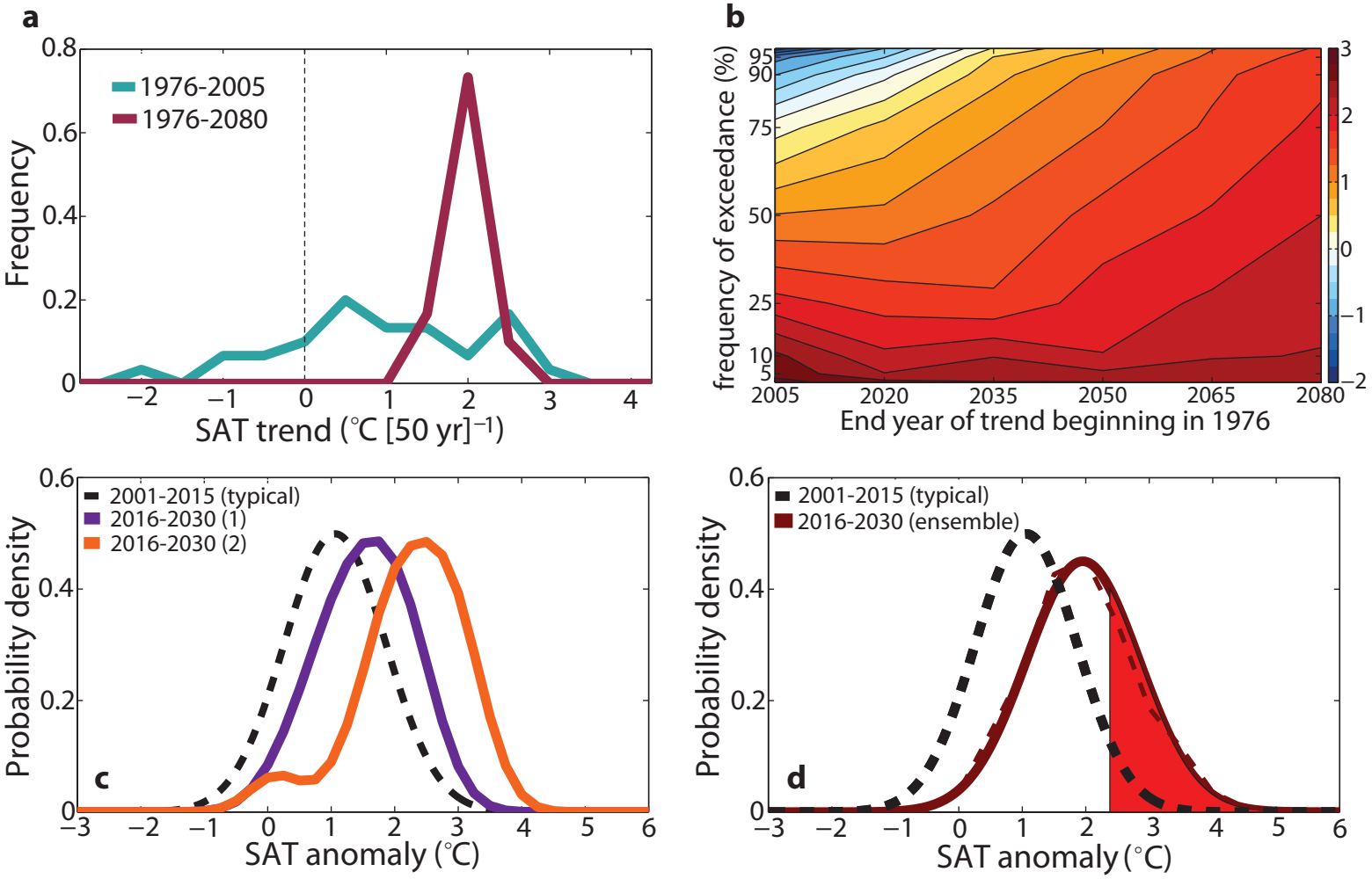
a
1976-2005
1976-2080
Frequency
SAT trend (°C [50 yr]⁻¹)
b
frequency of exceedance (%)
End year of trend beginning in 1976
c
2001-2015 (typical)
2016-2030 (1)
2016-2030 (2)
Probability density
SAT anomaly (°C)
d
2001-2015 (typical)
2016-2030 (ensemble)
Probability density
SAT anomaly (°C)

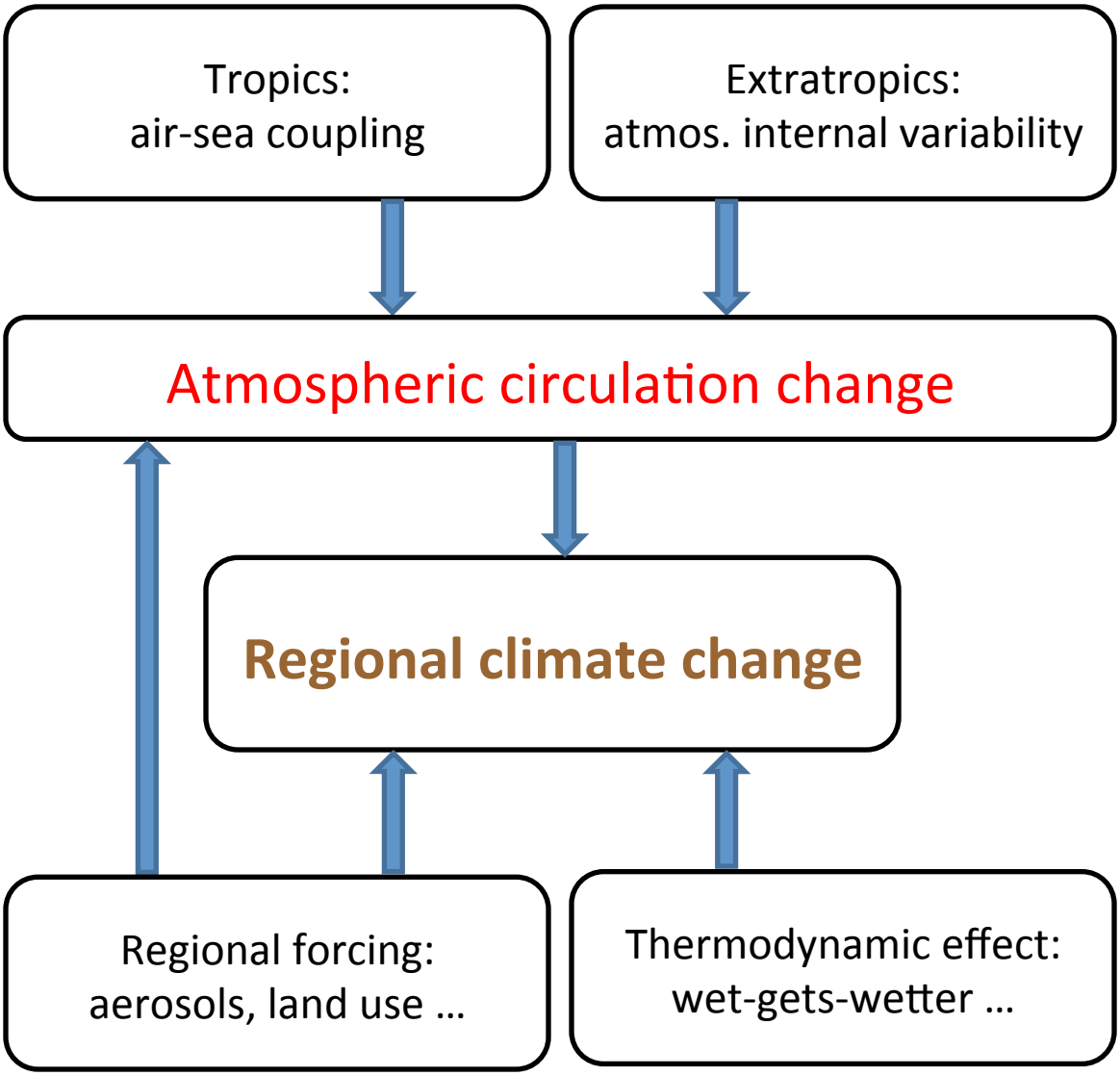
Tropics:
air-sea coupling
Extratropics:
atmos. internal variability
Atmospheric circulation change
Regional climate change
Regional forcing:
aerosols, land use …
Thermodynamic effect:
wet-gets-wetter …

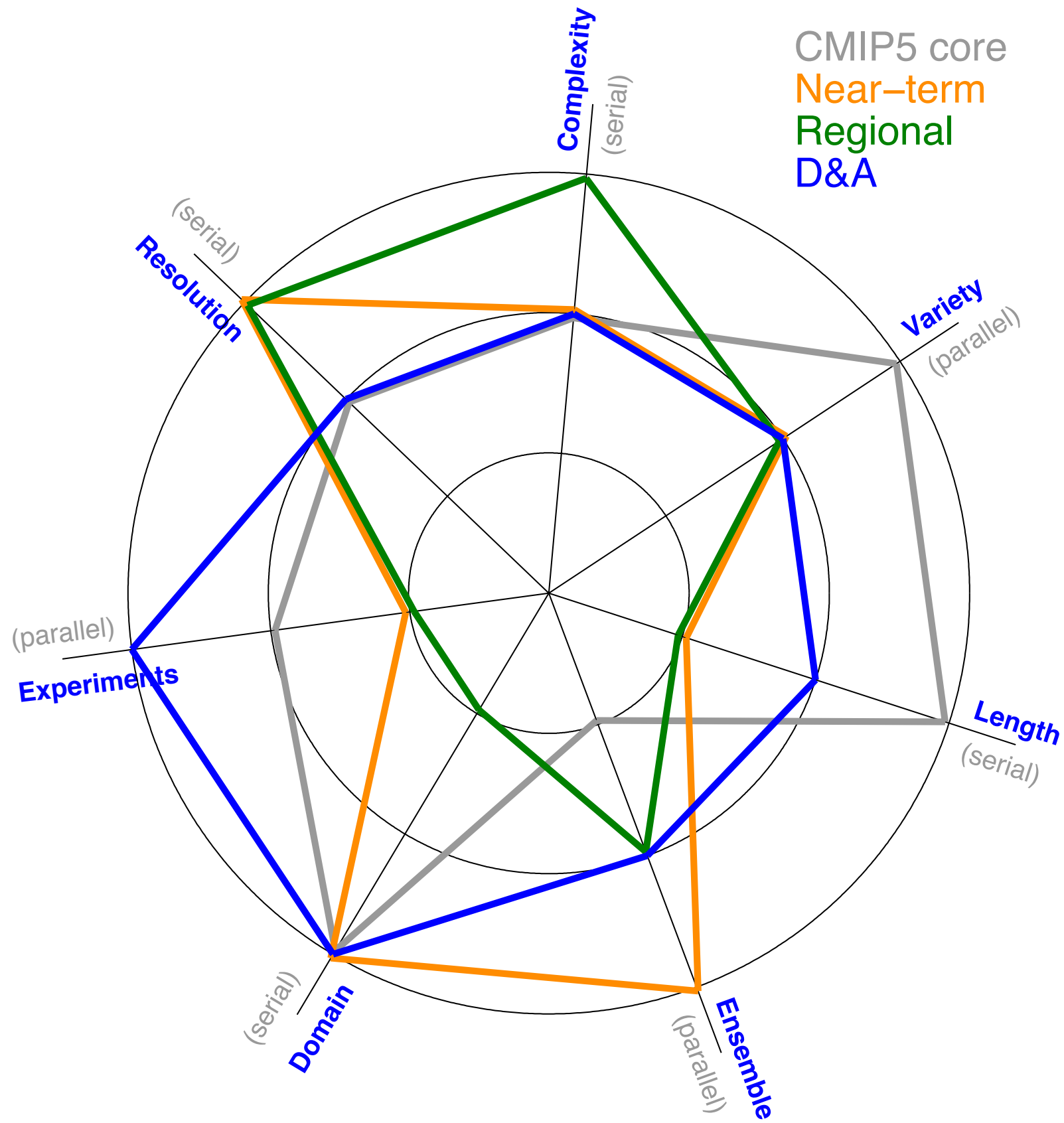
CMIP5 core
Near–term
Regional
D&A
Complexity
(serial)
Variety
(parallel)
Length
(serial)
Ensemble
(parallel)
Domain
(serial)
Experiments
(parallel)
Resolution
(serial)